

## Isothermal Pyrolysis of Low-Rank Coal: Kinetic Study, Batch Experiments, and Product Analysis

Pabitra Mohan Mahapatra , Maneesh Acharya , Narayan Gouda , Gayatri Sabat , Achyut Kumar Panda\*

1. Department of Chemistry, Veer Surendra Sai University of Technology, Burla, Odisha, India. E-mail: pmmahapatra\_phdchem@vssut.ac.in
2. Department of Chemistry, Veer Surendra Sai University of Technology, Burla, Odisha, India. E-mail: maneeshacharya8@gmail.com
3. Department of Chemistry, School of Applied Sciences, Centurion University of Technology and Management, Paralakhemundi, Odisha, India. E-mail: gouda24narayan@gmail.com
4. Department of Chemistry, Veer Surendra Sai University of Technology, Burla, Odisha, India. E-mail: gayatri.sabat@gmail.com
5. Department of Chemistry, Veer Surendra Sai University of Technology, Burla, Odisha, India. E-mail: akpanda\_chem@vssut.ac.in

ARTICLE INFO	ABSTRACT
<p><b>Article History:</b> Received: 26 January 2025 Revised: 18 June 2025 Accepted: 30 June 2025 Published: 30 June 2025</p> <p><b>Article type:</b> Research</p> <p><b>Keywords:</b> Batch Pyrolysis, Isothermal Pyrolysis, Low-Rank Coal, Model-Fitting, Pyrolysis Index</p>	<p>Effective use of low-grade coal is crucial for meeting global energy needs and mitigating environmental impacts, making the study of its thermal decomposition a key focus for sustainable energy development. Understanding the pyrolytic degradation process of coal is crucial for optimizing its use in eco-friendly energy solutions. It is hypothesized that the isothermal pyrolysis of low-rank coal at different temperatures will exhibit different kinetic behaviors and produce valuable condensable products. This research investigates the pyrolytic behavior, kinetics, and batch pyrolysis of low-rank coal. Thermo-gravimetric analysis was conducted under isothermal conditions at temperatures ranging from 350 to 500 °C, with a 25 °C increment, for 2 hours in an inert atmosphere. The data were analyzed using model-fitting methods, testing a total of 21 models to calculate the reaction kinetics. The results revealed that weight loss increased with temperature, reaching a maximum at 18.61% (450 °C), with activation energies of 5.817–123.51 kJ/mol. The D2 diffusion model best described the process (<math>E_a = 7.267</math> kJ/mol, <math>A = 0.022</math> min<sup>-1</sup>). The pyrolysis index rose from 0.0113 (350 °C) to 0.051 (500 °C). At 450°C, 18.9% condensable products formed, containing alkanes, alicyclics, and aromatics (FTIR/GC-MS). These findings facilitate the optimization of sustainable pyrolysis of low-rank coal for the production of valuable outputs.</p>

## Introduction

Compared to other fossil fuels, coal is more affordable, available, and plentiful. Many nations, including India, the United States, China, and Australia, have experienced a financial boom due to the presence of coal reserves [1]. In 2022–23, India produced 893.190 MT of raw coal, marking a 14.77% increase from 778.210 MT in 2021–22. Odisha led coal production in 2022–23 with 218.981 MT, followed by Chhattisgarh (184.895 MT), Jharkhand (156.445 MT), and Madhya Pradesh (146.028 MT) [2]. India obtains 55% of its energy from coal [3].

\* Corresponding Author: A.K. Panda (E-mail address: akpanda\_chem@vssut.ac.in)



Additionally, coal is used in various industries, including the sponge iron industry, cement industry, fertilizers industry, chemicals industry, and steel industry, among others [4]. Thus, the marketable primary energy utilization in India has increased by more than 700% during the previous 40 years [5]. India has large deposits of low-grade coal [6]. Lignite is a low-grade coal with minimal carbon content [7]. Lignite production in India during 2022–23 was 44.990 MT, a 5.27% decrease from 47.492 MT in 2021–22. Lignite deposits in India are primarily located in the Tertiary sediments of the Southern and Western Peninsular Shield, particularly in Tamil Nadu, Pondicherry, Gujarat, Rajasthan, and Jammu & Kashmir, with smaller quantities also found in Odisha, Kerala, and West Bengal. The top lignite producers during 2022–23 were Tamil Nadu with 22.480 MT, Gujarat with 12.313 MT, and Rajasthan with 10.197 MT [2]. The direct use of these coals for energy generation is unsuitable due to their poor energy yield and harmful environmental and health impacts. Therefore, developing sustainable and eco-friendly methods for coal conversion is essential to address the growing energy needs. Pyrolysis of such coal could produce high-energy-density liquid and gaseous fuel along with coke [6]. The successful transformation of low-rank coal into high-energy fuels requires a comprehensive understanding of its thermal decomposition characteristics and reaction kinetics.

Several studies on the non-isothermal kinetics of coal have been reported, summarized below. Dwivedi et al. pyrolyzed three samples of Indian coal in the range of 30–950 °C temperature and 50, 100, 150, and 200 K/min heating rates, in a nitrogen atmosphere. The activation energy ( $E_a$ ) value of Indian coal determined by the Friedman Method is 49.132 kJ/mol [6]. Research by Sabat et al. [8] examined the thermal decomposition kinetics of three coal grades (10, 13, and 14) under varying heating rates, employing first-order reaction models to determine average activation energies. The activation energy values calculated for Grade 10, Grade 13, and Grade 14 coal are 62.114, 61.940, and 57.563 kJ/mol, respectively [8]. Dong et al. performed pyrolysis of various Indian coals at heating rates ranging from 278 to 773 K/min and reported that the activation energy of the Indian coals ranged from 428.78 to 520 kJ/mol, as computed using the Friedman method [9]. Prabhakar et al. pyrolyze the coal fines under non-isothermal conditions in a nitrogen atmosphere at 20, 30, and 40 °C/min heating rates and reported the activation energy ( $E_a$ ) (31.41 kJ/mol to 50.42 kJ/mol) and Arrhenius factor ( $A$ ) value ( $1.05 \times 10^6$  to  $1.4 \times 10^7 \text{ min}^{-1}$ ) calculated by using the isoconversional method [10]. Research by Yan et al. demonstrated that thermal decomposition progressively converts aliphatic carbon into aromatic structures in subbituminous coals, with both cluster size and molecular weight growing with coal rank. Concurrently, the activation energy distribution narrowed as rank increased [11]. Casa et al. reported that among different coal types, lignite showed the lowest pyrolysis activation energy (73 kJ/mol), whereas anthracite exhibited the highest (138 kJ/mol). Bituminous coal displayed intermediate values between 97 and 117 kJ/mol [12]. According to Guo et al., increasing the heating rate results in higher initial and final reaction temperatures, with a significant impact on coal pyrolysis. The highest  $E_a$  is found in the 850–930 °C temperature range. The lowest activation energy is observed at a heating rate of 15 °C/min. Greater hydrogen production occurs when coal is heated at a rate of 15 °C/min in a fixed-bed reactor [13]. Ashraf et al. [14] investigated the thermal degradation behavior of CC and DC coals under non-isothermal conditions, applying heating rates ranging from 10–40 °C/min (in 10 °C intervals). The average  $E_a$  values for CC and DC were calculated using the Friedman differential isoconversional model, yielding values of 134.54 and 129.81 kJ/mol, respectively [14]. Gao et al. observed that both the activation energy ( $E_a$ ) and pre-exponential factor ( $A$ ) increased proportionally with the heating rate during coking coal pyrolysis. Their study found these parameters remained unaffected by particle size variations, and noted that coking coal consistently demonstrated higher  $E_a$  values compared to non-coking varieties [15].

While non-isothermal techniques have dominated solid-state kinetic analysis for decades, isothermal methods are increasingly preferred due to their practical advantages. Unlike dynamic heating approaches, isothermal analysis simplifies kinetic parameter determination by eliminating temperature gradients and non-stationary heat transfer effects. By maintaining constant temperature conditions, this method allows more straightforward identification of reaction mechanisms and orders, as it avoids the complexities introduced by varying heating rates in non-isothermal experiments [16]. A few reports on the isothermal kinetic analysis of coal, as reported in the literature, are summarized as follows.

Jeong et al. investigated the pyrolysis of coking coal blended with biomass using both non-isothermal and isothermal methods in a thermogravimetric analyzer. For non-isothermal pyrolysis, heating rates of 5, 10, 15, and 20 °C/min were applied from 25 °C to 800 °C, while isothermal pyrolysis was performed between 500–800 °C. The study found that weak coking coal (WCC) exhibited higher activation energy (252.08–579.4 kJ/mol) compared to hard coking coal (HCC) (163.7–272.45 kJ/mol) under non-isothermal conditions. Additionally, HCC/biomass blends had lower activation energies (88.71–400.98 kJ/mol) than WCC/biomass blends (127.7–456.44 kJ/mol). Increasing the biomass proportion in the blends reduced activation energy for both coal types. Under isothermal conditions, the activation energies for WCC and HCC blended with biomass were 42 kJ/mol and 40 kJ/mol, respectively [17]. Zhang et al. studied the pyrolysis kinetics of coal and oil shale under isothermal and non-isothermal conditions using a microfluidized bed analyzer. Their findings revealed that the kinetic parameters, including activation energy ( $E_a$ ) and pre-exponential factor ( $A$ ), differed significantly between gas components. Notably, oil shale exhibited higher  $E_a$  and  $A$  values compared to both coal types [18]. Maria et al. examined the pyrolysis behavior of two Spanish coals (Mequinenza and Samca) under both isothermal (400, 500, and 600 °C) and non-isothermal conditions (heating rates of 5, 15, and 30 °C/min). Their results showed that isothermal runs had notably lower correlation coefficients compared to non-isothermal experiments. During non-isothermal pyrolysis, the mean activation energies for  $H_2S$  and  $CO_2$  were lower than those for  $CH_4$  and  $CO$  in both coals, though this trend did not hold under isothermal conditions. The study also found that activation energies varied based on coal type, pyrolysis conditions (isothermal vs. non-isothermal), and temperature [19].

The literature review reveals a gap in the detailed isothermal kinetic studies of low-rank coal, particularly those incorporating batch pyrolysis and product characterization. In our earlier research, first-order model fitting was employed to thoroughly investigate the non-isothermal pyrolytic degradation behavior, kinetics, and thermodynamics of low-rank Indian coal across varying grades and heating rates [8, 20]. It was confirmed that grade 10 coal is the most optimal, with the primary non-isothermal thermal degradation zone occurring between 350 °C and 500 °C. Most studies in the literature typically use heating rates ranging from 1 to 20 °C/min for kinetic analysis [21]. Building on previous research, this study investigates the pyrolysis kinetics of Grade 10 low-rank Indian coal under isothermal conditions, spanning a temperature range of 350–500 °C in 50 °C increments at a heating rate of 20 °C/min. In addition to kinetic analysis, batch pyrolysis experiments were conducted to characterize the chemical composition of condensable pyrolytic products. The key contribution of this work lies in its comprehensive assessment of both kinetic and thermodynamic parameters during the isothermal decomposition of low-rank coal, coupled with detailed analysis of the pyrolysis oil products.

## Material and methods

### Coal Sample

The grade 10 low-rank Indian coal sample [8] for this work is collected from the Mahanadi Coal Fields Ltd., Sambalpur, Odisha. The coal sample is ground using a household grinder and

then filtered to a grid size of 100 meshes (0.149 mm). Then, the required-sized coal is dehydrated by heating for 48 hours at 40 °C in air.

### Characterizations of Coal

Coal sample characterization was conducted following ASTM standards: moisture (ASTM D4442), volatile matter (ASTM D3172), ash (ASTM D3175), and fixed carbon (ASTM D3177). Ultimate analysis (CHNS/O content) was performed using a Vario El III CHNS analyzer (Germany) with flash combustion at 1200°C, helium carrier gas, and thermal conductivity detection. Calorific value was determined via bomb calorimetry (ASTM D5865-12). Non-isothermal pyrolysis (30–900°C, 20°C/min, 20 ml/min N<sub>2</sub>) and isothermal pyrolysis (375–500°C, two h hold, 20 ml/min N<sub>2</sub>) were conducted in a Pyris STA 8000 TGA. Samples (~9.5 mg) were heated to target temperatures at a rate of 40°C/min for isothermal tests. All experiments were triplicated to ensure reproducibility.

### Batch Pyrolysis Study and Product Analysis

The batch reactor used in this experiment is described in our previous work [20], consisting of a stainless steel tube with an outlet tube at one end to collect the cracked products. The pyrolysis reactor consisted of a stainless steel tube with a length of 145 mm and an internal diameter of 37 mm (external diameter: 41 mm). An external electric furnace provided heating with temperature regulation achieved through a Shimaden PID controller ( $\pm 3.6^\circ\text{C}$  accuracy). Real-time temperature monitoring was performed using a K-type Cr-Al thermocouple installed inside the reactor chamber. The optimal pyrolysis experimental temperature for yielding the maximum condensable fraction is determined by experimenting with different temperatures ranging from 400 to 600 °C and found to be 450 °C [8].

For each pyrolysis trial, 30 g of coal was processed at 450°C in the reactor system. The liquid products were condensed using a 20°C water-cooled condenser and subsequently weighed; the solid residue was measured after pyrolysis. Gas yields were determined through mass balance calculations, with all experiments conducted in triplicate for reproducibility.

The condensed oils underwent comprehensive analysis using:

1. FTIR spectroscopy (Bruker Alpha, 500–4000 cm<sup>-1</sup> range, 2 cm<sup>-1</sup> resolution) with ZnSe ATR accessory for functional group identification.
2. High-resolution GC-TOFMS (AccuTOF GCV, 10–2000 amu range, 6000 amu resolution) for precise compositional determination.

### Isothermal Kinetic Analysis

Isothermal kinetic analysis using model-fitting methods allows accurate determination of the kinetic triplet: reaction mechanism, activation energy, and pre-exponential (Arrhenius) factor. This research applied a model-fitting approach, incorporating four fundamental kinetic models: nucleation, geometrical contraction, diffusion, and reaction-order models. Nucleation models describe the formation and growth of new phases at imperfections in the crystal lattice, such as dislocations or impurities, and may involve complex multi-step processes. Geometrical contraction models assume that decomposition begins at the surface and progresses inward as a shrinking core, with the rate governed by the movement of the reaction front. Diffusion models, on the other hand, are based on the transport of volatile or reactive species through product layers and typically describe slower processes due to increasing diffusion resistance. Reaction-order models follow classical kinetics, where the reaction rate depends on the concentration or conversion degree raised to a defined order [22].

The rate equation for the solid-state reaction [23]:

$$\frac{d\alpha}{dt} = k f(\alpha) \Rightarrow \frac{d\alpha}{f(\alpha)} = k dt \quad (1)$$

We know,

$$\alpha = (m_0 - m_t)/(m_0 - m_f) \quad (2)$$

On integrating Eq. 1

$$\int_0^\alpha \frac{d\alpha}{f(\alpha)} = \int_0^t k dt \Rightarrow g(\alpha) = k t + C \quad (3)$$

The value of the rate constant  $k$  at a definite temperature can be determined from the plot of  $g(\alpha)$  and  $t$  based on the maximum coefficient of determination ( $R^2$ ).

According to Arrhenius's equation:

$$\ln k = \ln A - \frac{E_a}{RT} \quad (4)$$

The values of activation energy ( $E_a$ ) and the pre-exponential factor ( $A$ ) can be calculated using the slope and intercept from the linear graph of  $\ln k$  versus  $1/T$ . Table 1 lists the corresponding  $f(\alpha)$  and  $g(\alpha)$  functions [24] for various solid-state reaction mechanisms.

**Table 1.** Value of the differential and integral functions of solid-state kinetic models

Model	Symbol	$f(\alpha)$	$g(\alpha)$
Model of Nucleation Power Law	P2	$2\alpha^{1/2}$	$\alpha^{1/2}$
	P3	$3\alpha^{2/3}$	$\alpha^{1/3}$
	P4	$4\alpha^{3/4}$	$\alpha^{1/4}$
	P3/2	$(3/2)\alpha^{1/3}$	$\alpha^{2/3}$
Model of Nucleation Avrami Erofev	A2	$2(1-\alpha) [-\ln(1-\alpha)]^{1/2}$	$[-\ln(1-\alpha)]^{1/2}$
	A3	$3(1-\alpha) [-\ln(1-\alpha)]^{2/3}$	$[-\ln(1-\alpha)]^{1/3}$
	A4	$4(1-\alpha) [-\ln(1-\alpha)]^{3/4}$	$[-\ln(1-\alpha)]^{1/4}$
Model of Geometric Contraction	R2	$2(1-\alpha)^{1/2}$	$1-(1-\alpha)^{1/2}$
	R3	$3(1-\alpha)^{2/3}$	$1-(1-\alpha)^{1/3}$
Model of Diffusion	D1	$(1/2)\alpha^{-1}$	$\alpha^2$
	D2	$[-\ln(1-\alpha)]^{-1}$	$(1-\alpha) \ln(1-\alpha) + \alpha$
	D3	$(3/2)(1-\alpha)^{2/3}[1-(1-\alpha)^{1/3}]^{-1}$	$[1-(1-\alpha)^{1/3}]^2$
	D4	$(3/2)[(1-\alpha)^{-1/3}-1]^{-1}$	$1-(2/3)\alpha-(1-\alpha)^{2/3}$
Model of Reaction Order	F0	1	$\alpha$
	F1	$1-\alpha$	$[-\ln(1-\alpha)]$
	F1.5	$(1-\alpha)^{3/2}$	$2[(1-\alpha)^{-1/2}-1]$
	F2	$(1-\alpha)^2$	$[\alpha/(1-\alpha)]$
	F2.5	$(1-\alpha)^{2.5}$	$(2/3)[(1-\alpha)^{-3/2}-1]$
	F3	$(1-\alpha)^3$	$(1/2)[(1-\alpha)^{-2}-1]$
	F4	$(1-\alpha)^4$	$(1/3)[(1-\alpha)^{-3}-1]$
	F5	$(1-\alpha)^5$	$(1/4)[(1-\alpha)^{-4}-1]$

The pyrolysis index (I) is:

$$I = \frac{(dw/dt)_{\max}}{t_{\max} \Delta t} \quad (5)$$

Where,  $t_{\max}$  = Time at maximum reaction rate in minutes,  $(dw/dt)_{\max}$  = Maximum weight loss rate in percent per minute,  $\Delta t$  = Required amount of time in minutes for the primary reaction, and mathematically it is given:

$$\Delta t = t_f - t_i$$

where,  $t_i$  = Time in min at  $\alpha = 0.05$ ,  $t_f$  = Time in min at  $\alpha = 0.95$ .



## Result Analysis

### Characterization of Coal

#### *Proximate, Ultimate, and Calorimetric Analysis*

From the findings of the proximate analysis, it is inferred that coal contains 24.44 % volatile chemicals, 4.16 % moisture, 44.4 % ash, and 27 % fixed carbon, respectively. The ultimate analysis reveals that it contains no nitrogen, 0.344% sulfur, 2.38% hydrogen, 38.81% carbon, 58.466% oxygen, and other metallic components. The gross calorific value of coal is 3138.01 cal/g. Coal has a moisture content that requires energy to be removed before it can be processed. The volatile content of coal leads to the production of condensable gases, resulting in a yield of liquid and waxy products [25]. The fixed carbon content yields the production of carbonaceous products. The high ash content in coal increases handling and processing costs, decreases the rate of combustion, carbonization, and pyrolysis, and affects the efficiency of metallurgical applications [25, 26]. Therefore, during pyrolysis, a high amount of residue is formed. The elevated carbon and hydrogen content in coal contributes to the formation of more aromatic compounds in pyrolytic products, whereas the higher oxygen content results in the formation of more oxygenated compounds. Coal degradation does not release  $\text{NO}_x$ ; however, the sulfur present (0.344%) can still contribute to the release of  $\text{SO}_x$  during thermal degradation. The lower calorific value of coal is due to its higher ash, moisture, and oxygen content [25].

#### *Pyrolytic Degradation Behavior*

The thermal degradation behavior of the coal sample is studied from the thermogravimetric analysis (TGA). The thermogravimetric (TG) and derivative thermogravimetric (DTG) profiles of the coal sample are presented in Fig. 1. These measurements were conducted under non-isothermal conditions, with a heating rate of 20 °C/min over a temperature range of 30 to 900 °C.

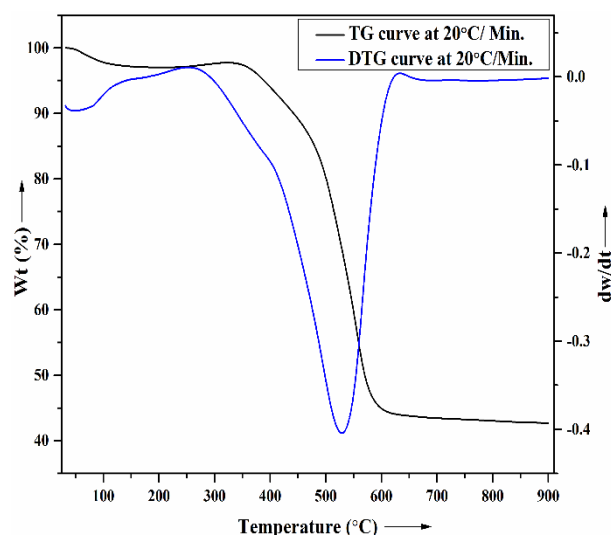


Fig. 1. TG-DTG plot of the coal sample at heating rate 20 °C/min

From Fig. 1, it is clear that the pyrolysis of the coal sample in the temperature range of 30-900 °C is completed in three zones, including (i) drying of moisture and removal of volatile components, (ii) degradation and devolatilization of degradation products or pyrolysis stage,

(iii) solid decomposition or polycondensation heated under non-isothermal conditions. The physi-adsorbed water and highly volatile matter present in the coal are released in the first stage (30-250 °C) with a weight loss of 2.75 %. In the second zone, a prominent peak in the DTG curve is observed at a temperature range of 250-630 °C, corresponding to a weight loss of 53.45%, which is attributed to the thermal degradation and release of volatile components and lighter fractions. In the third zone, a negligible weight of 1.05% occurs, corresponding to the release of CO<sub>2</sub> due to the degradation of carbonates in coal and the production of H<sub>2</sub> due to the condensation of aromatic rings in biochar [8]. Therefore, during the pyrolysis of coal under non-isothermal conditions, the total weight loss is approximately 57.25%. The significant weight loss for the coal occurs within the 250-630 °C temperature range. Thus, to investigate the reaction kinetics under isothermal conditions, experiments were performed at seven distinct temperatures: 350, 375, 400, 425, 450, 475, and 500 °C.

Fig. 2 presents the TG-DTG curves obtained from the isothermal pyrolysis of the coal sample at constant temperatures as specified above. The analysis reveals a two-stage pyrolytic degradation process: (1) initial non-isothermal decomposition (first peak) and (2) subsequent isothermal decomposition (second peak).

Before reaching the target temperature, the coal undergoes partial degradation under non-isothermal conditions. Once the desired temperature is achieved, isothermal degradation dominates. However, due to the finite heat-up period in TG analysis, actual isothermal conditions are never instantaneously attained, making complete isolation of isothermal degradation unfeasible. This inherent non-isothermal phase must be accounted for in isothermal thermogravimetric experiments [27].

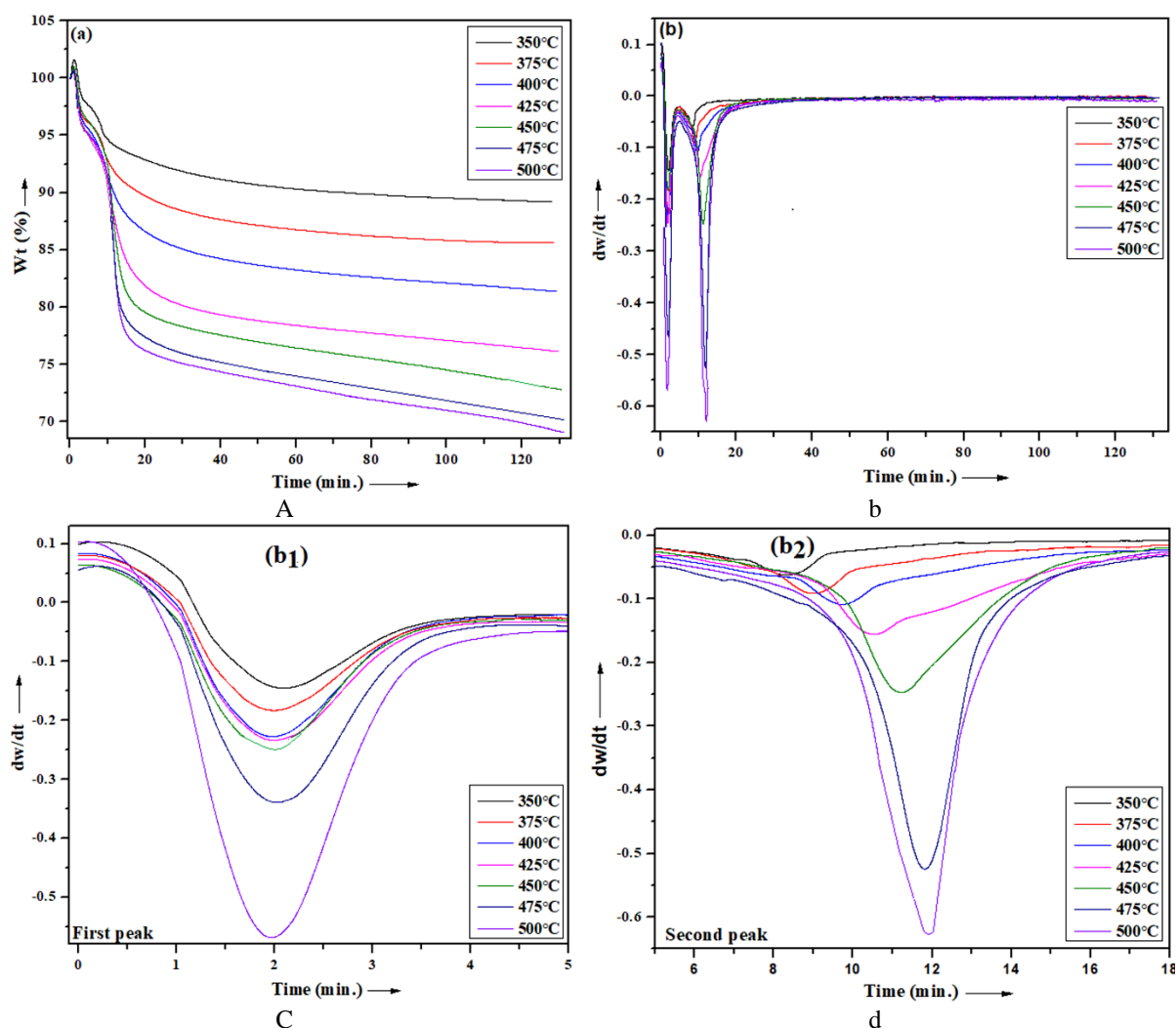


Fig. 2. Isothermal (a) TG curve, (b) DTG curve, (c) 1st peak, and (d) 2nd peak in DTG curve

Analysis of the thermogravimetric experimental result at different constant temperatures (Fig. 2) reveal that the onset of isothermal pyrolysis occurred at various time intervals for each temperature: 8 min (350 °C), 8.625 min (375 °C), 9.25 min (400 °C), 9.875 min (425 °C), 10.5 min (450 °C), 11.125 min (475 °C), and 11.75 min (500 °C). Table 2 summarizes the weight loss characteristics corresponding to both degradation peaks and the total pyrolysis process.

**Table 2.** Isothermal pyrolysis weight loss of the coal sample

Temperature (°C)	Weight loss (%)		Total weight loss (%)
	First peak	Second peak	
350	4.000	6.832	10.832
375	5.690	8.670	14.360
400	7.422	11.196	18.618
425	8.400	15.403	23.803
450	8.680	18.610	27.290
475	13.390	16.460	29.850
500	16.355	15.605	31.960

From Table 2, two main stages of degradation can be observed, namely (i) the first Stage (Non-Isothermal): between 350-500 °C, the rate of weight loss shows a consistent upward trend with temperature. (ii) Second Stage (Isothermal): The weight loss goes up until 450 °C (reaching 18.61%) but then starts decreasing at higher temperatures.

However, overall weight loss continues to increase with temperature, with the highest loss (31.96%) occurring at 500 °C. This means that while the second stage slows down after 450 °C, the total decomposition still improves at higher temperatures.

### Isothermal Kinetic Analysis

The isothermal degradation kinetics of coal were evaluated using multiple solid-state reaction models, as detailed in Table 1. The kinetic parameters were determined using TG data obtained under isothermal conditions. The kinetics of isothermal coal degradation are explained using various solid-state models, as summarized in Table 1. Plotting  $g(\alpha)$  versus time (Eq. 3) enables calculation of the rate constant  $k$ , with the most suitable kinetic model being chosen according to the most significant coefficient of determination ( $R^2$ ). Analysis of the data presented in Table 3 reveals that the  $D_2$  diffusion model provides the most accurate representation of isothermal degradation kinetics of the coal, as evidenced by its highest regression coefficient ( $R^2 = 0.940$ ). Fig. 3 shows the model-fitting plots for the diffusion models. Equivalent graphical representations can be constructed for nucleation models, geometrical contraction models, and reaction order mechanisms, with these plots serving as the basis for determining rate constants ( $k$ ) in subsequent activation energy ( $E_a$ ) calculations.



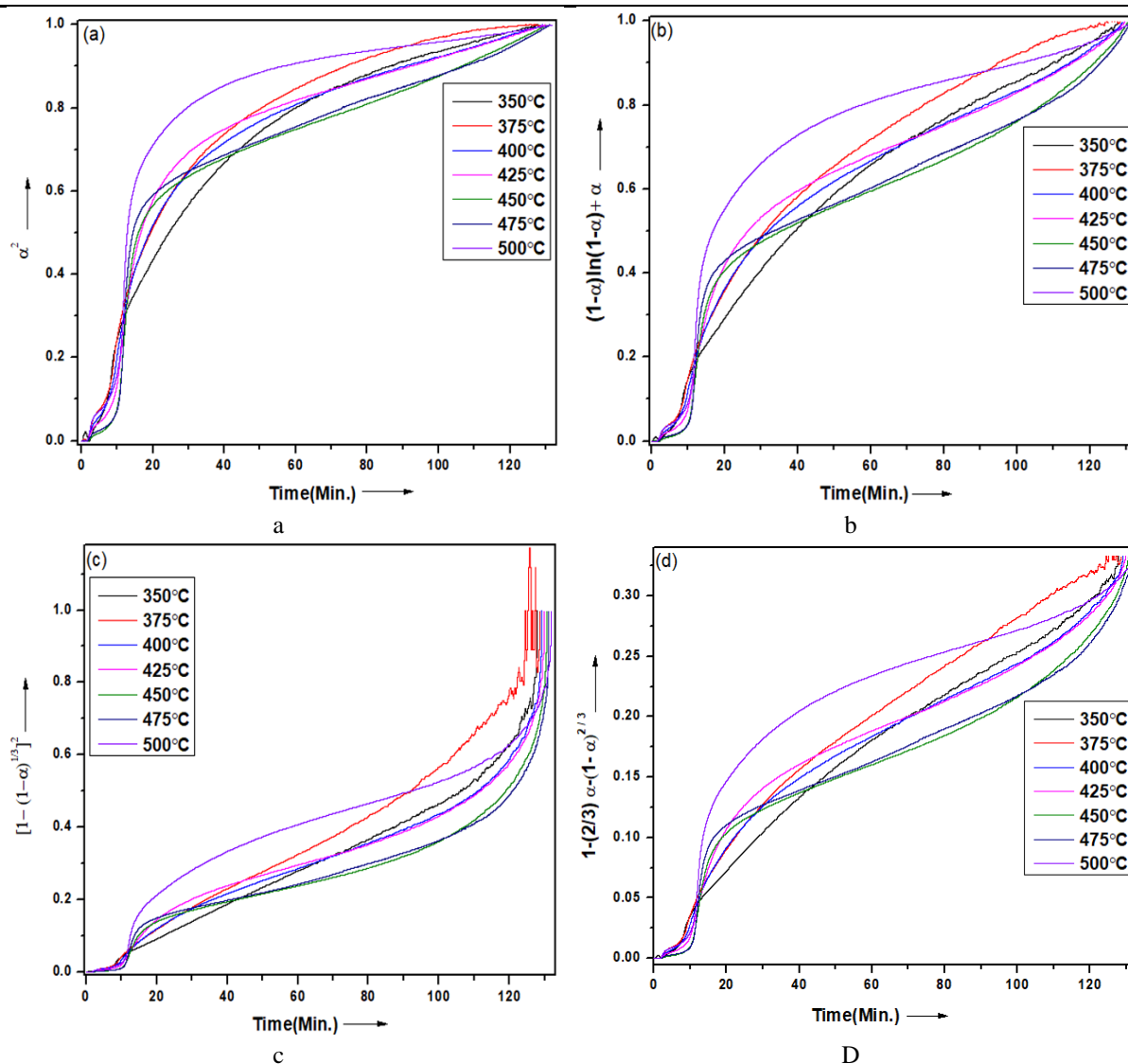


**Fig. 3.** Model fitting plots for diffusion model: (a)  $D_1$ , (b)  $D_2$ , (c)  $D_3$ , and (d)  $D_4$

The derived rate constant ( $k$ ) enables determination of activation energy ( $E_a$ ) and pre-exponential factor ( $A$ ) through Arrhenius analysis, achieved by plotting  $\ln k$  against reciprocal temperature ( $1/T$ ) as described in Eq. 4. As illustrated in Fig. 4, the temperature dependence of rate constants ( $\ln k$  vs.  $1/T$ ) was analyzed for each kinetic model (nucleation, geometrical contraction, diffusion, and reaction order), yielding the  $E_a$  and  $A$  parameters summarized in Table 3.

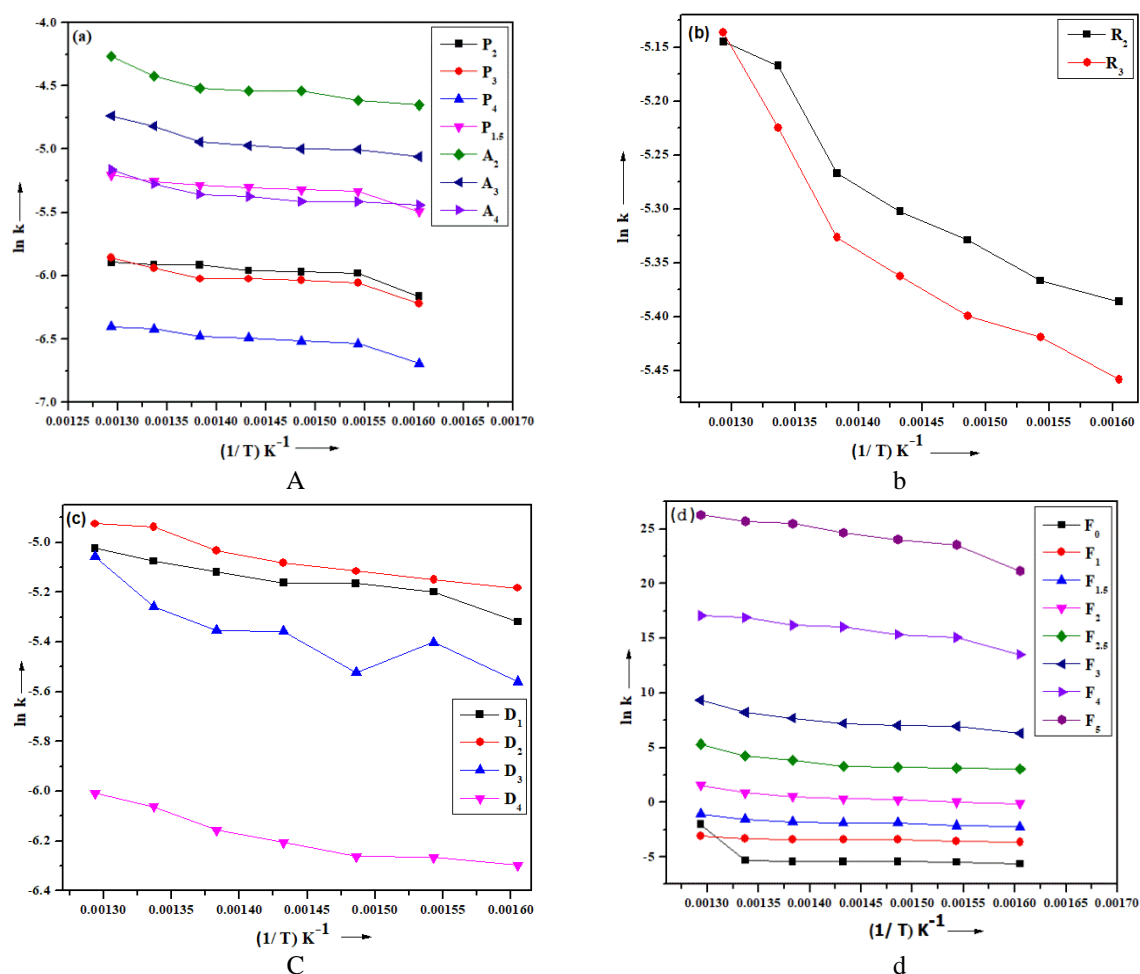


**Fig. 4.** Linear model fitting kinetic plots for (a) nucleation model, (b) contracting area model, (c) diffusion model, and (d) reaction order model

**Table 3.** Kinetic parameters from different models

Model	Reaction Model	R <sup>2</sup>	Ea (kJ/mol)	A(min <sup>-1</sup> )
Nucleation Model	P <sub>2</sub>	0.706	5.817	0.007
	P <sub>3</sub>	0.821	7.605	0.009
	P <sub>4</sub>	0.850	6.680	0.005
	P <sub>1.5</sub>	0.014	6.164	0.806
	A <sub>2</sub>	0.810	8.794	0.051
	A <sub>3</sub>	0.812	7.791	0.028
	A <sub>4</sub>	0.770	12.760	0.300
Geometrical Contraction Model	R <sub>2</sub>	0.911	6.695	0.016
	R <sub>3</sub>	0.868	8.025	0.019
Diffusion Method	D <sub>1</sub>	0.921	6.783	0.019
	D <sub>2</sub>	0.940	7.267	0.022
	D <sub>3</sub>	0.732	11.008	0.032
	D <sub>4</sub>	0.893	7.791	0.008
Reaction Order Model	F <sub>0</sub>	0.270	60.191	236.633
	F <sub>1</sub>	0.857	12.759	0.300
	F <sub>1.5</sub>	0.830	26.964	17.765
	F <sub>2</sub>	0.829	39.657	1.591×10 <sup>3</sup>
	F <sub>2.5</sub>	0.708	53.041	4.043×10 <sup>3</sup>
	F <sub>3</sub>	0.857	70.221	3.582×10 <sup>8</sup>
	F <sub>4</sub>	0.930	87.827	2.727×10 <sup>13</sup>
	F <sub>5</sub>	0.907	123.516	7.738×10 <sup>19</sup>

Based on this optimal model, the calculated activation energy and Arrhenius frequency factor for the process are 7.267 kJ/mol and  $0.022 \text{ min}^{-1}$ , respectively. It should be noted that activation energy values obtained from alternative kinetic models show considerable variation, ranging from 5.817 to 123.51 kJ/mol.

Nucleation models are too simple. The models assume the material is uniform and conditions are ideal. In reality, materials often contain impurities and have uneven structures. Temperature and pressure can change rapidly, which is not accounted for in the models. Nucleation also focuses too much on thermodynamics and overlooks the rapidity of changes. Due to this, nucleation models are not effective for complex processes, such as coal pyrolysis. The Geometrical Contraction Model fails because it oversimplifies reaction dynamics, particularly in complex systems such as coal pyrolysis, where the material undergoes significant structural changes. The model assumes uniform shrinking of the unreacted core and a predictable inward-moving reaction front. In reality, reactions involve the formation of porous structures, changes in surface areas, and diffusion limits, which the model overlooks. In coal pyrolysis, the production of gas and liquid products can create internal pressure, altering porosity and causing uneven shrinkage. The model also assumes a constant reaction rate, while real systems experience variable rates due to temperature gradients, concentration changes, and material heterogeneity. These factors make the model unreliable for non-uniform or dynamic processes. The Reaction Order Model often fails because it oversimplifies complex chemical processes, especially when reaction mechanisms are unclear or involve multiple steps. It assumes the reaction rate depends solely on reactant concentrations raised to a fixed power, which is inaccurate in systems where pathways change over time or under varying conditions. In processes like coal pyrolysis, intermediate steps, such as diffusion or chemical rearrangements, are not captured by a simple rate equation. The model also assumes constant activation energy and a uniform mechanism, which do not hold in heterogeneous systems with temperature gradients or varying material properties. This leads to significant differences between predicted and actual behavior. The diffusion method is often successful because it accurately reflects how reactions are controlled by the movement of reactants or products, especially in systems with porous materials, like coal. In processes like coal pyrolysis, the chemical reaction might happen quickly, but the rate at which gases or reactants can move through the material often limits the overall reaction rate. Diffusion models account for this, explaining why reactions slow down over time. These models also align more closely with experimental observations, particularly when the activation energy is lower, suggesting that diffusion, rather than chemical reactions, is the rate-limiting step [28].

The high ash content in coal reduces its energy density, as ash is inert and does not contribute to the pyrolysis process. It also impedes heat and mass transfer, which can increase the activation energy required for thermal degradation. Despite this, the relatively low activation energy calculated in this study may be attributed to the high volatile matter and fixed carbon contents, which enhance reactivity. Volatile matter facilitates the release of fuel gases and accelerates reaction rates, while fixed carbon supports sustained combustion [25]. Moreover, the low activation energy aligns with a diffusion-controlled mechanism, as diffusion processes typically require less energy than chemical reaction-limited steps, supporting the applicability of the  $D_2$  diffusion model to coal pyrolysis [28]. Table 4 presents the kinetic results for various low-rank coals under different experimental conditions.

**Table 4.** Kinetic results of different low-rank coals

Low-Rank Coal	Kinetic Method	Experimental Conditions	Ea (kJ/mol)	A (min <sup>-1</sup> )	Ref.
Grade-10	Model-fitting	Temperature = 375, 400, 425, 450, 475, and 500 °C, Heating rate = 40 °C/min, Reaction time = 2 h, and Nitrogen flow rate = 20 mL/min	7.267	0.022	Current study
Grade-10 Grade-13 Grade-14	Coats Redfern	Temperature range = 30–1000 °C, Heating rate = 5, 10, 15, 20, and 25 °C/min, and Nitrogen flow rate = 40 mL/min	62.114 61.940 57.563	5.190×10 <sup>5</sup> 3.655×10 <sup>5</sup> 4.257×10 <sup>4</sup>	[8]
Indian low-grade coal	Friedman	Temperature range = 30–950 °C, Heating rate = 50, 100, 150, and 200 K/min, Nitrogen flow rate = 40 mL/min	49.132	188.88	[6]
Chinese western low-rank coal	Pseudo-first order	Temperature range = 25–500 °C, Heating rate = 10, 20, and 30 °C/min, and Nitrogen flow rate = 100 mL/min	113.170	7.975×10 <sup>9</sup>	[15]
Indian high-ash coal	Friedman	Temperature range = Room temperature to 1173 K, Heating rate = 278, 293, 323, 373, 573, 773 K/min, and Nitrogen flow rate = 60 mL/min	428.78–520	2.920×10 <sup>36</sup>	[9]
Shenhua coal	Coats–Redfern	Temperature range = Room temperature to 900 °C, Heating rate = 10, 15, and 20 °C/min, and Nitrogen flow rate = 40 mL/min	140.44	1.737×10 <sup>15</sup>	[13]
Lignite NCC LFC (Heilongjiang) LFC (Shandong)	Distributed activation energy model	Temperature range = Room temperature to 1050 °C, Heating rate = 5, 10, 20, and 30 °C/min, and Nitrogen flow rate = 50 mL/min	331 298 302 196	----- ----- ----- -----	[29]
Lignite NCC LFC (Heilongjiang) LFC (Shandong)	Doyle's integral method	Temperature range = Room temperature to 1050 °C, Heating rate = 10 °C/min, and Nitrogen flow rate = 50 mL/min	37.97 40.40 48.59 42.4	240.20 195.62 4645.45 1204.27	[30]
Lignite and subbituminous coal	Kissinger, KAS, FWO, Friedman	Temperatures range = 298–1173 K, Heating rate = 1, 6, 9, 12, 15, and 18 K/min, and Nitrogen flow rate = 100mL/min	281, 282, 275, 283	2.61×10 <sup>17</sup> , 2×10 <sup>20</sup> , 1.07×10 <sup>27</sup> , 1.89×10 <sup>23</sup>	[31]

## Pyrolysis Index

The maximum pyrolysis rate and reaction time influence the pyrolysis index. In terms of reaction rate, a higher pyrolysis index indicates better pyrolysis performance [23]. The pyrolysis index for coal at different temperatures is calculated using Eq. 5 and listed in Table 5.

**Table 5.** Pyrolysis index

<b>First Peak</b>					
<b>T (°C)</b>	<b>t<sub>i</sub> (min)</b>	<b>t<sub>max</sub> (min)</b>	<b>t<sub>f</sub> (min)</b>	<b>DTG<sub>max</sub> (% min<sup>-1</sup>)</b>	<b>I (% min<sup>-3</sup>)</b>
350	2.20	2.10	4.62	14.38	2.830
375	1.80	2.09	4.44	18.24	3.306
400	1.72	2.05	4.43	22.67	4.081
425	1.66	2.03	4.38	23.29	4.218
450	1.54	1.99	4.28	24.98	4.582
475	1.53	1.98	4.25	33.87	6.289
500	1.49	1.97	4.15	56.80	10.839
<b>Second Peak</b>					
350	6.12	8.35	72.96	6.30	0.011
375	6.44	9.01	83.26	9.02	0.013
400	6.57	9.72	85.31	10.81	0.014
425	6.92	10.55	100.59	15.46	0.016
450	7.04	11.24	101.45	24.67	0.023
475	7.32	11.59	110.37	52.36	0.044
500	7.69	11.92	112.71	62.87	0.051

Due to the DTG curve having two peaks, the pyrolysis index for the sample cannot be precisely calculated. The first peak corresponds to non-isothermal degradation, but the second peak corresponds to isothermal degradation. Therefore, the pyrolysis index variation in the first peak concerning time parameters ( $t_i$ ,  $t_{max}$ , and  $t_f$ ) is contradictory to that in the second peak. The pyrolysis index for first-stage degradation increases with increases in temperature from 350 °C to 500 °C. However, for this work, the second stage of degradation plays an important role, which also increases from 350 °C to 500 °C. According to Table 5, the second step of the pyrolytic degradation of coal results in much better pyrolysis performance at 500 °C than at other temperatures.

### Batch Pyrolysis Results

From the isothermal kinetic analysis, it is observed that the maximum degradation occurs at 450 °C. Thus, the batch pyrolysis experiment is carried out at this temperature to obtain the condensable fraction. Different products, viz. the condensable fraction (18.9 %), the non-condensable fraction (1.9 %), and the residue (79.2 %), are formed during the experiment. The condensable fraction is a dark, black-coloured liquid. The high ash content in coal results in the formation of a substantial amount of residue during thermal processing [25]. The reaction time for the batch pyrolysis of low rank coal is 95 minutes. Fig. 5 illustrates the relationship between the pyrolytic fraction and the yield.

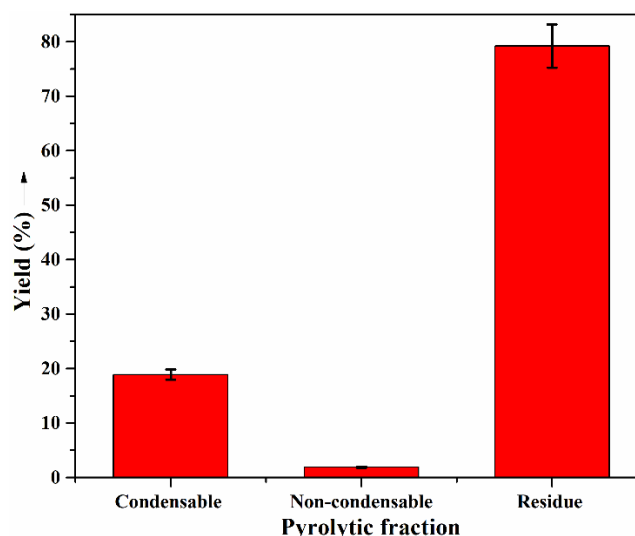


**Fig. 5.** Plot of pyrolytic product distribution

#### *Composition of Pyrolytic Oil Using GC-MS and FTIR*

The composition of the liquid fraction is confirmed using GC-MS and FTIR analysis. The Gas chromatography-mass spectrometry plot for the oil formed at 450 °C during the pyrolysis of coal under isothermal conditions is represented in [Fig. 6](#).

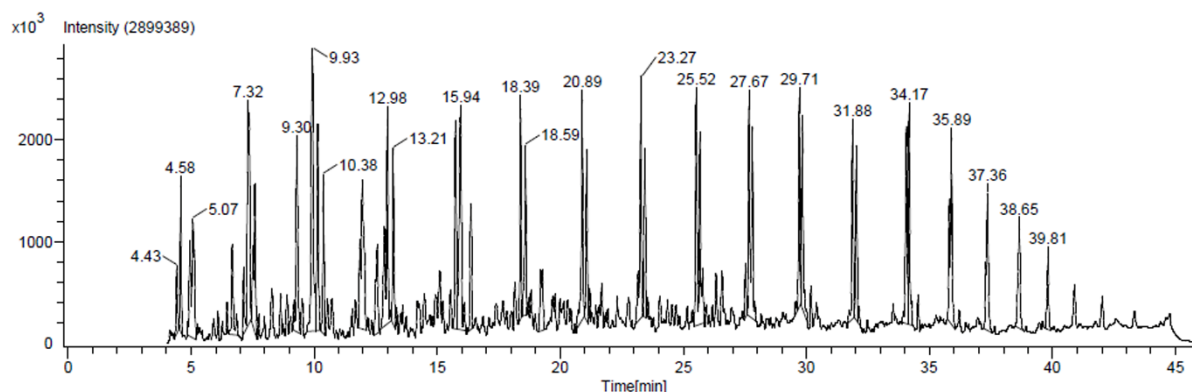


**Fig. 6.** GC-MS plot of the coal pyrolytic oil @ 450 °C

[Table 6](#) lists the compounds present in the pyrolytic oil, as determined by GC-MS analysis. Three different categories of compounds, including aliphatic alkanes, alicyclic compounds, and aromatic compounds, are identified in the oil. The aliphatic alkanes constitute 16.48 % of pyrolytic oil with C<sub>15</sub>-C<sub>21</sub>. Heptadecane has the most significant area percentage among all aliphatic alkanes at 11.23 %, in addition to pentadecane and octadecane. The oil contains 35.25% alicyclic compounds with a carbon chain length of C<sub>12</sub>-C<sub>15</sub>, with D-Limonene (28.45%) having the highest area percentage among the alicyclic compounds. The third and highest fraction among the three categories is aromatic compounds (48.27%), with a range of carbon chain lengths from C<sub>6</sub> to C<sub>20</sub>. The majority of the components in this category include phenol and its derivatives, with 4-methylphenol (12.05 %) having the highest area percentage.



**Table 6.** GC-MS component analysis of coal pyrolytic oil

Compound	Molecular Formula	Area %
<b>(1) Aliphatic alkane</b>		<b>16.48</b>
Heptadecane	C <sub>17</sub> H <sub>36</sub>	11.23
Pentadecane	C <sub>15</sub> H <sub>32</sub>	2.20
Octadecane	C <sub>18</sub> H <sub>38</sub>	1.70
2,6,10,15-tetramethyl heptadecane	C <sub>21</sub> H <sub>44</sub>	1.35
<b>(2) Alicyclic Compound</b>		<b>35.25</b>
D-Limonene	C <sub>10</sub> H <sub>16</sub>	28.45
3,7,7-trimethyl-11-methylene spiro [5.5] undec-2-ene	C <sub>15</sub> H <sub>24</sub>	3.74
7,7-dimethyl bicyclo [3.1.1] hept-3-ene-spiro-2,4-(1,3-dioxane)	C <sub>12</sub> H <sub>18</sub> O <sub>2</sub>	3.06
<b>(3) Aromatic compound</b>		<b>48.27</b>
4-methyl phenol	C <sub>7</sub> H <sub>8</sub> O	12.05
Phenol	C <sub>6</sub> H <sub>6</sub> O	8.17
2,4-dimethyl phenol	C <sub>8</sub> H <sub>10</sub> O	7.75
2-methyl phenol	C <sub>7</sub> H <sub>8</sub> O	6.25
o-[(1,2,3,4-tetrahydro-2-naphthyl) methyl] hydro cinnamic acid	C <sub>20</sub> H <sub>22</sub> O <sub>2</sub>	5.82
1,1(1,3-propanediyl) bisbenzene	C <sub>15</sub> H <sub>16</sub>	3.88
1-ethyl-2,3-dihydro-1-methyl-1H-Indene	C <sub>12</sub> H <sub>16</sub>	2.47
1-ethylidene-1H-Indene	C <sub>11</sub> H <sub>10</sub>	1.88

The FTIR spectrum of the oil obtained from coal pyrolysis at 450 °C is presented in [Fig. 7](#). Key absorption peaks are observed at 1726 cm<sup>-1</sup> (C=O stretching), 1216 cm<sup>-1</sup> (C-O stretching), and 720 cm<sup>-1</sup> (O-H out-of-plane bending), which are characteristic of carboxylic acid functional groups. These findings align with the identification of o-[(1,2,3,4-tetrahydro-2-naphthyl)methyl] hydrocinnamic acid in [Table 6](#), confirming its presence in the pyrolytic oil. The FTIR spectrum also exhibits characteristic peaks at 2920 cm<sup>-1</sup> (asymmetric C-H stretching of methylene groups), 2850 cm<sup>-1</sup> (symmetric C-H stretching of methylene groups), 909 cm<sup>-1</sup> (C=C stretching), 1473 cm<sup>-1</sup> (asymmetric CH<sub>3</sub> bending), and 1376 cm<sup>-1</sup> (symmetric CH<sub>3</sub> bending). These absorption bands indicate the presence of long-chain aliphatic hydrocarbons in the pyrolytic oil, which is further corroborated by GC-MS analysis. The FTIR spectrum displays characteristic peaks at 1603 cm<sup>-1</sup>, attributed to C=C skeletal vibrations and aromatic ring stretching, and at 1376 cm<sup>-1</sup>, associated with in-plane bending vibrations. These absorption bands indicate the presence of phenolic compounds in the pyrolytic oil. Additionally, the peak observed at 720 cm<sup>-1</sup>, corresponding to out-of-plane bending, further supports the existence of phenol derivatives, such as 4-methylphenol, 2,4-dimethylphenol, and 2-methylphenol. These findings are consistent with the compound identification obtained through GC-MS analysis. The absorption band at 909 cm<sup>-1</sup> can be attributed to out-of-plane bending vibrations, potentially indicating the presence of alicyclic structures. This spectral feature suggests that compounds such as D-limonene, 3,7,7-trimethyl-11-methylene-spiro[5.5]undec-2-ene, and 7,7-dimethylbicyclo [3.1.1]hept-3-ene-spiro-2,4-(1,3-dioxane) may be present in the sample [\[32\]](#).

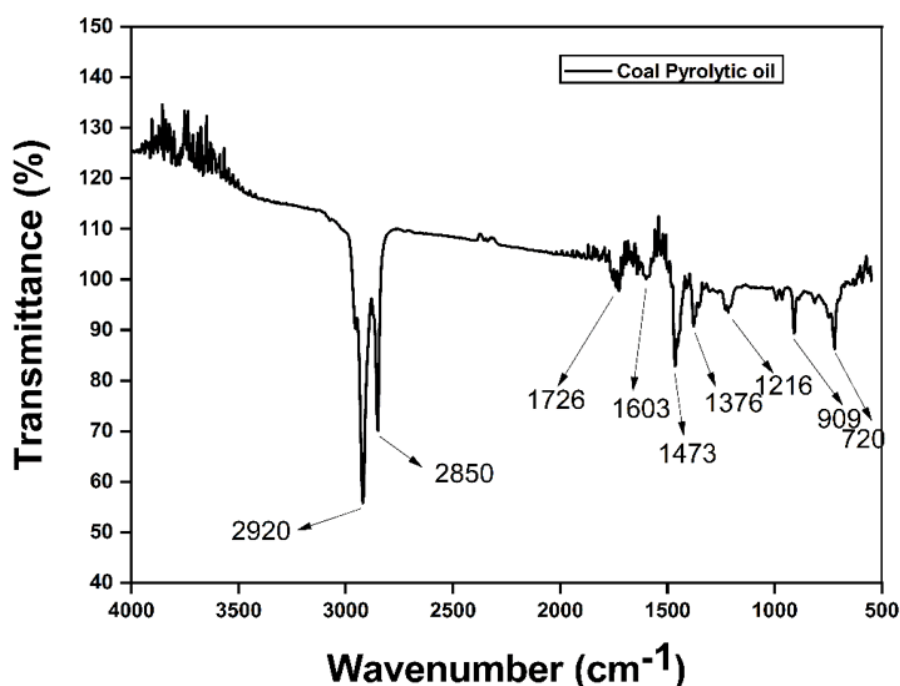


Fig. 7. FTIR plot of the coal-derived pyrolytic oil produced at 450 °C

## Conclusion

The pyrolytic degradation behaviors and kinetics of coal under isothermal conditions are studied using the TGA technique. Model-fitting kinetic equations related to different mechanisms are used to calculate the kinetic parameters. There is a noticeable increase in overall weight loss in isothermal conditions with rising temperatures. The maximum % weight loss under isothermal conditions is 18.61 % at 450 °C. The activation energy for the reaction ranges between 5.817 and 123.51 kJ/mol, depending on the model used. Under isothermal conditions, coal pyrolysis degradation best fits the D2 diffusion model, yielding an activation energy ( $E_a$ ) of 7.267 kJ/mol and a pre-exponential factor ( $A$ ) of 0.022 min<sup>-1</sup>, based on the criterion of the highest regression coefficient ( $R^2$ ). Aliphatic alkanes, including heptadecane, pentadecane, octadecane, and heptadecane, are detected in addition to alicyclic and aromatic compounds in the pyrolytic oil produced by the isothermal pyrolysis of coal at 450 °C. Using effective methods, the pyrolytic mixture products may be separated into usable compounds.

## Nomenclature

### Roman Symbols

Roman Symbol	Definition	Unit
A	Arrhenius constant	minute <sup>-1</sup>
C	Integration constant	----
$E_a$	Activation energy	kJ/mol
I	Pyrolysis index	% min <sup>-3</sup>
K	Rate constant	minute <sup>-1</sup>
M	Mass	Mg
R	Gas constant	kJmol <sup>-1</sup> K <sup>-1</sup>
$R^2$	Coefficient of determination	----
T	Reaction time	Minute

T	Temperatures	°C, and K
W	Weight	mg, and g
$f(\alpha)$	Function of the differential reaction mechanism	----
$g(\alpha) = \int_0^\alpha \frac{d\alpha}{f(\alpha)}$	Integral form of the mechanism	-----
$\frac{d\alpha}{dt}$	Rate of Reaction	Moles l <sup>-1</sup> s <sup>-1</sup>
$m_0$	Initial mass	G
$m_t$	Instantaneous mass at a specific time t	G
$m_f$	Final mass	G
<b>Greek Letters</b>		
A	Degree of Conversion	----

## Abbreviation

ASTM	American Society for Testing and Materials
ATR	Attenuated Total Reflectance
CC	Chamalang Coal
CHNS	Carbon, Hydrogen, Nitrogen, Sulphur
CI	Chemical Ionization
DC	Dukki Coal
DLATGA	Deuterated L-alanine doped triglycene sulphate
DTG	Differential Thermogravimetry
EI	Electron Ionization
FTIR	Fourier Transform Infrared
FWO	Flynn-Wall-Ozawa
GC-MS	Gas chromatography-mass spectrometry
GCV	Gas Chromatography-Vacuum
HCC	Hard coking coal
KAS	Kissinger-Akahira-Sunose
LFC	Long-flame coal
MCL	Mahanadi Coalfields Limited
MS	Mass Spectrometer
NCC	Non-caking coal
OPUS	Online-Publikationsverbund der Universität Stuttgart
PID	Proportional – Integral – Derivative
STA	Simultaneous Thermal Analyzer
TGA	Thermogravimetry analysis
TOF	Time-of-flight
WCC	Weak coking coal

## Acknowledgments

We sincerely acknowledge TEQIP-III, VSSUT, Burla, for providing the instrumental facilities necessary to characterize the samples in this research.

## Data Availability

The corresponding author may be requested to provide data availability information.

## Declarations

### Ethical Approval

Not applicable.

### Consent to Participate

All the authors gave consent to participate.

### Consent for Publication

All the authors gave explicit consent to submit the work to the Journal of Chemical and Petroleum Engineering.

## Funding

The authors declare that no funds, grants, or other forms of support were received during the course of this work.

## Competing Interests

The authors declare no relevant financial or non-financial interests.

## References

- [1] Balat M. Coal in the global energy scene. *Energy Sources, Part B: Economics, Planning, and Policy*. 2009 Dec 28;5(1):50-62. <https://doi.org/10.1080/15567240701758927>
- [2] Provisional coal statistics 2022-23, Ministry of Coal, Government of India. Date of access: 29<sup>th</sup> April 2025. <https://coal.nic.in/sites/default/files/2023-10/17-10-2023a-wn.pdf>
- [3] Qaisar SH, Ahmad MA. Production, consumption and future challenges of coal in India. *International Journal of Current Engineering and Technology*. 2014;4(5):3437-40. <https://citeseerx.ist.psu.edu/document?repid=rep1&type=pdf&doi=529d147a661b3de112c2a931582737f953b33440>
- [4] Coal in India, Date of access :3rd October 2022. [https://en.wikipedia.org/wiki/Coal\\_in\\_India](https://en.wikipedia.org/wiki/Coal_in_India)
- [5] Ramkumar M, Santosh M, Mathew MJ, Siddiqui NA. India at crossroads for energy. *Geoscience Frontiers*. 2021 Nov 1;12(6):100901. <https://doi.org/10.1016/j.gsf.2019.10.006>
- [6] Dwivedi KK, Chatterjee PK, Karmakar MK, Pramanick AK. Pyrolysis characteristics and kinetics of Indian low rank coal using thermogravimetric analysis. *International Journal of Coal Science & Technology*. 2019 Mar;6:102-12. <https://doi.org/10.1007/s40789-019-0236-7>
- [7] Unlocking Transparency by Third Party Assessment of Mined Coal, UTTAM, Ministry of Coal, Government of India, Date of access: 29<sup>th</sup> April 2025. <https://uttam.coalindia.in/about.html#:~:text=Lignite:%20It%20is%20the%20lowest,Nadu%2C%20and%20Jammu%20&%20Kashmir>
- [8] Sabat G, Gouda N, Panda AK. Effect of coal grade and heating rate on the thermal degradation behavior, kinetics, and thermodynamics of pyrolysis of low-rank coal. *International Journal of Coal Preparation and Utilization*. 2023 Jun 3;43(6):1057-75. <https://doi.org/10.1080/19392699.2022.2096013>
- [9] Dong L, Vuthaluru H, French D, Karmakar S, Sutrar AK, Satyakam R. Indian coal pyrolysis behaviour and kinetics study using covalent bond information. *Thermochimica Acta*. 2022 May 1;711:179208. <https://doi.org/10.1016/j.tca.2022.179208>

- [10] Prabhakar A, Sadhukhan AK, Gupta P. Study of pyrolysis kinetics of coal fines using model free method. *Materials Today: Proceedings*. 2022 Jan 1;68:910-5. <https://doi.org/10.1016/j.matpr.2022.07.079>
- [11] Yan J, Liu M, Feng Z, Bai Z, Shui H, Li Z, Lei Z, Wang Z, Ren S, Kang S, Yan H. Study on the pyrolysis kinetics of low-medium rank coals with distributed activation energy model. *Fuel*. 2020 Feb 1;261:116359. <https://doi.org/10.1016/j.fuel.2019.116359>
- [12] Casal MD, Vega MF, Diaz-Faes E, Barriocanal C. The influence of chemical structure on the kinetics of coal pyrolysis. *International Journal of Coal Geology*. 2018 Jul 1;195:415-22. <https://doi.org/10.1016/j.coal.2018.06.014>
- [13] Guo Z, Zhang L, Wang P, Liu H, Jia J, Fu X, Li S, Wang X, Li Z, Shu X. Study on kinetics of coal pyrolysis at different heating rates to produce hydrogen. *Fuel processing technology*. 2013 Mar 1;107:23-6. <https://doi.org/10.1016/j.fuproc.2012.08.021>
- [14] Ashraf A, Sattar H, Munir S. Thermal decomposition study and pyrolysis kinetics of coal and agricultural residues under non-isothermal conditions. *Fuel*. 2019 Jan 1;235:504-14. <https://doi.org/10.1016/j.fuel.2018.07.120>
- [15] Gao Z, Zheng M, Zhang D, Zhang W. Low-temperature pyrolysis properties and kinetics of non-coking coal in Chinese western coals. *Journal of the Energy Institute*. 2016 Nov 1;89(4):544-59. <https://doi.org/10.1016/j.joei.2015.07.002>
- [16] Vyazovkin S, Wight CA. Isothermal and non-isothermal kinetics of thermally stimulated reactions of solids. *International reviews in physical chemistry*. 1998 Jul 1;17(3):407-33. <https://doi.org/10.1080/014423598230108>
- [17] Jeong HM, Seo MW, Jeong SM, Na BK, Yoon SJ, Lee JG, Lee WJ. Pyrolysis kinetics of coking coal mixed with biomass under non-isothermal and isothermal conditions. *Bioresource technology*. 2014 Mar 1;155:442-5. <https://doi.org/10.1016/j.biortech.2014.01.005>
- [18] Zhang Y, Zhao M, Linghu R, Wang C, Zhang S. Comparative kinetics of coal and oil shale pyrolysis in a micro fluidized bed reaction analyzer. *Carbon Resources Conversion*. 2019 Dec 1;2(3):217-24. <https://doi.org/10.1016/j.crcon.2019.10.001>
- [19] Lazaro MJ, Moliner R, Suelves I. Non-isothermal versus isothermal technique to evaluate kinetic parameters of coal pyrolysis. *Journal of Analytical and Applied Pyrolysis*. 1998 Oct 1;47(2):111-25. [https://doi.org/10.1016/S0165-2370\(98\)00083-7](https://doi.org/10.1016/S0165-2370(98)00083-7)
- [20] Sabat G, Gouda N, Panda AK. Pyrolysis of low-rank coal: Thermo-kinetic analysis and product characterization. *Environmental Quality Management*. 2022 Dec;32(2):73-83. <https://doi.org/10.1002/tqem.21911>
- [21] Vyazovkin S, Chrissafis K, Di Lorenzo ML, Koga N, Pijolat M, Roduit B, Sbirrazzuoli N, Sunol JJ. ICTAC Kinetics Committee recommendations for collecting experimental thermal analysis data for kinetic computations. *Thermochimica Acta*. 2014;590:1–23. <https://doi.org/10.1016/j.tca.2014.05.036>
- [22] Mahapatra PM, Gouda N, Pradhan D, Mishra PC, Mishra P, Panda AK. Isothermal co-pyrolytic kinetics investigation of polystyrene/polymethyl methacrylate blended Bakelite. *Canadian Journal of Chemical Engineering*. <https://doi.org/10.1002/cjce.25505>
- [23] Hu DH, Chen MQ, Huang YW, Wei SH, Zhong XB. Evaluation on isothermal pyrolysis characteristics of typical technical solid wastes. *Thermochimica Acta*. 2020 Jun 1;688:178604. <https://doi.org/10.1016/j.tca.2020.178604>
- [24] Sahoo A, Kumar S, Mohanty K. Kinetic and thermodynamic analysis of Putranjiva roxburghii (putranjiva) and Cassia fistula (amaltas) non-edible oilseeds using the thermogravimetric analyzer. *Renewable Energy*. 2021 Mar 1;165:261-277. <https://doi.org/10.1016/j.renene.2020.11.011>
- [25] Mahapatra PM, Kumar S, Mishra P, Panda AK. Effect of different thermoplastics on the thermal degradation behavior, kinetics, and thermodynamics of discarded bakelite. *Environmental Science and Pollution Research*. 2024;31(27):38788–38800. <https://doi.org/10.1007/s11356-023-25953-2>
- [26] Sharma S, Ghoshal AK. Study of kinetics of co-pyrolysis of coal and waste LDPE blends under argon atmosphere. *Fuel*. 2010;89:3943–3951. <https://doi.org/10.1016/j.fuel.2010.06.033>

- [27] Vyazovkin S, Burnham AK, Criado JM, Pérez-Maqueda LA, Popescu C, Sbirrazzuoli N. ICTAC Kinetics Committee recommendations for performing kinetic computations on thermal analysis data. *Thermochimica Acta*. 2011 Jun 10;520(1-2):1-9. <https://doi.org/10.1016/j.tca.2011.03.034>
- [28] Ammar Khawam and Douglas R. Flanagan, *The Journal of Physical Chemistry B* 2006 110 (35), 17315-17328, <https://doi.org/10.1021/jp062746a>
- [29] Song H, Liu G, Wu J. Pyrolysis characteristics and kinetics of low-rank coals by distributed activation energy model. *Energy Conversion and Management*. 2016;126:1037–1046. <https://doi.org/10.1016/j.enconman.2016.08.082>
- [30] Song H, Liu G, Zhang J, Wu J. Pyrolysis characteristics and kinetics of low-rank coals by TG-FTIR method. *Fuel Processing Technology*. 2017;156:454–460. <https://doi.org/10.1016/j.fuproc.2016.10.008>
- [31] Heydari M, Rahman M, Gupta R. Kinetic study and thermal decomposition behavior of lignite coal. *International Journal of Chemical Engineering*. 2015;2015:Article ID 481739, 9. <https://doi.org/10.1155/2015/481739>
- [32] Sharma, Y. R. *Elementary organic spectroscopy*. S. Chand Publishing. 2007.

**How to cite:** Mahapatra P.M, Acharya M, Gouda N, Sabat G, Panda A.K. Isothermal Pyrolysis of Low-Rank Coal: Kinetic Study, Batch Experiments, and Product Analysis. *Journal of Chemical and Petroleum Engineering* 2025; 59(2): 271-290.